

Article

Effect of the Solvent Type on the Colloidal Stability and the Degree of Condensation of Silica Sols Stabilized by Amphiphilic Urethane Acrylate and the Properties of Their Coating Films

Hong Nhung Le ^{1,†}, Choonho Lee ^{2,†}, Woochul Jung ² and Juyoung Kim ^{1,*} 

¹ Nanocomposite Structure Polymer Laboratory, Department of Advanced Materials Engineering, Kangwon National University, Samcheok 25913, Republic of Korea; hongnhungle94@kangwon.ac.kr

² Interior and Exterior Material Development Team, Hyundai Motor Company, Hwasung-si 18280, Republic of Korea; chlee0561@hyundai.com (C.L.); sub3285@hyundai-ngv.com (W.J.)

* Correspondence: juyoungk@kangwon.ac.kr

† These authors contributed equally to this work.

Abstract: The colloidal stability of silica O-I hybrid sols that have a high degree of condensation could result in the formation of a hard coating film on a substrate, which could depend on the properties of solvents used in the sol-gel reaction. In this study, the effect of the solvent type on the colloidal stability and degree of condensation of the silica sols was investigated by preparing various silica O-I hybrid sols using different solvent mixtures composed of various aprotic and protic solvents in the presence of amphiphilic urethane acrylate. Silica sols prepared using the appropriate aprotic-protic solvent mixture showed a higher degree of condensation and long-term colloidal stability, which was confirmed using ²⁹Si-NMR and DLS. Furthermore, the coating film formed from these silica sols showed a remarkable hardness of 0.97 GPa, with a thickness of 4.76 μm confirmed using nanoindentation measurements.

Keywords: sol-gel; aprotic solvent; protic solvent; hybrid; colloidal; amphiphilic polymer



Citation: Le, H.N.; Lee, C.; Jung, W.; Kim, J. Effect of the Solvent Type on the Colloidal Stability and the Degree of Condensation of Silica Sols Stabilized by Amphiphilic Urethane Acrylate and the Properties of Their Coating Films. *Coatings* **2023**, *13*, 1997. <https://doi.org/10.3390/coatings13121997>

Academic Editor: Dimitrios Tasis

Received: 2 November 2023

Revised: 22 November 2023

Accepted: 23 November 2023

Published: 24 November 2023



Copyright: © 2023 by the authors. Licensee MDPI, Basel, Switzerland. This article is an open access article distributed under the terms and conditions of the Creative Commons Attribution (CC BY) license (<https://creativecommons.org/licenses/by/4.0/>).

1. Introduction

Organic-inorganic (O-I) hybrid materials have emerged as a promising class of composite materials wherein organic and inorganic components are homogeneously dispersed at the nanometer or molecular level. The integration of organic and inorganic phases at this scale can lead to synergistic effects and novel functionalities that are unreachable with either of the components alone. To meet diverse application requirements, O-I hybrid materials with specific structures and morphologies, including nanorods [1–4], nanosheets [5], nanoparticles [6], and nanotubes [7], have been developed. One of the most attractive applications of these materials is their use as coatings for automotive components, space industry equipment, and electronic devices [8–10], where silica-based (SiO₂-based) O-I hybrid nanoparticles have recently been used as potential candidates [9,11,12].

The sol-gel process has been recognized as an effective wetting chemical technique for designing homogeneous and high-quality, ultrafine nanostructured O-I hybrid thin films for over two decades, owing to its ability to enable configurational and structural control simultaneously [12–14]. In this process, colloidal sols are formed through the hydrolysis-condensation reaction of an alkoxy inorganic precursor, which subsequently transforms into solid network gels during the curing step. The mechanical properties of the resulting coating film (solid gels), particularly its hardness, strongly depend on the degree of condensation (DOC) achieved during the hydrolysis-condensation reaction. A higher degree of condensation leads to a greater crosslinking density in the network, directly affecting the film's hardness [15]. Therefore, it is essential to carefully control parameters

such as the pH, choice of inorganic precursor, temperature, and other relevant factors that significantly affect the hydrolysis-condensation process.

Among them, the solvent is a crucial parameter in controlling the rate of the hydrolysis-condensation reaction and the degree of condensation, depending on the type of solvent (aprotic or protic) and its polarity [16–19]. The hydrolysis reaction follows the S_N2 reaction mechanism (favored under acidic conditions) or the S_N1 reaction mechanism (favored under basic conditions), both of which are strongly affected by the solvent used. For the condensation reaction, depending on the pH of the solution, aprotic or protic solvents can hinder or promote the condensation reaction by forming hydrogen bonds with either the protonated or deprotonated silanols, which are involved in the condensation mechanism. So far, in most of the studies analyzing the effect of the solvent on the hydrolysis-condensation reaction, a single solvent was used during the process [16–18,20,21]. To the best of our knowledge, a limited number of papers [16,19] have reported on the effect of a solvent mixture on the degree of condensation during the preparation of SiO_2 O-I hybrid nanoparticles and the hardness of the resulting coating films.

In this study, our primary focus was to investigate the effect of different solvent mixtures on the degree of condensation of the hydrolysis-condensation reaction during the preparation of the SiO_2 O-I hybrid nanoparticles. To achieve this, the SiO_2 O-I hybrid sols were prepared via the sol-gel process using an amphiphilic urethane acrylate nonionomer polymer as a stabilization agent, which was reported in our previous study [17], facilitating their dispersion in various organic solvent mixtures. Unlike typical stabilization agents that need to be eliminated after preparation to prevent mechanical property deterioration in O-I hybrid materials, the UAN 1000-1450 stabilizing agent enhanced colloidal stability and prevented aggregation during the sol-gel process. Additionally, the UAN 1000-1450 promoted the formation of a homogeneous film upon curing, resulting in increased mechanical properties of the coating film. The solvent mixtures consisted of aprotic solvents, namely methyl ethyl ketone (M) and cyclohexanone (C), along with protic solvents, specifically ethanol (E) and propylene glycol methyl ether (P). We studied the effect of the solvent mixtures on the hardness of the resulting coating film using the DOC results and boiling point data. Additionally, the effect of the solvent mixtures on the long-term stability of colloidal SiO_2 O-I hybrid nanoparticles was evaluated through dynamic light scattering measurements (DLS).

2. Materials and Methods

2.1. Materials

For the synthesis of the amphiphilic urethane nonionomer precursor (UAN 1000-1450), 2,4-toluene diisocyanate (TDI; $M_w = 174.2$ g/mol, Sigma-Aldrich Co., Louis, MO, USA), glycerol propoxylate (GP, $M_w = 1000$ g/mol, KPX Chemical Co., Seoul, Republic of Korea), 2-hydroxyethyl methacrylate (2-HEMA, $M_w = 130.143$ g/mol, Sigma-Aldrich Co., USA), and poly(ethylene glycol) (PEG, $M_w = 1450$ g/mol, Sigma-Aldrich Co., USA) were used as received. Acetone (Sigma-Aldrich Co., USA) was used as a solvent without further purification. Furthermore, in the preparation of organic-inorganic hybrid solutions, tetraethyl orthosilicate (TEOS; $M_w = 208.33$ g/mol, Sigma-Aldrich Co., USA) was utilized as the inorganic precursor. Methyl ethyl ketone (MEK, Sigma Aldrich, USA), ethanol (Sigma-Aldrich Co., USA), propylene glycol methyl ether (PGME, Daejung Chemical Co., Siheung, Republic of Korea), and cyclohexanone (CY, Daejung Chemical Co., Republic of Korea) were used as solvents without further purification. To simplify the naming of the solvent mixtures, the solvents, including MEK, CY, PGME, and ethanol, are denoted by the symbols M, C, P, and E, respectively, throughout the manuscript. These solvents were categorized into two distinct groups: group A and group B. Group A consisted of the solvents used in the polymerization of the UAN 1000-1450, while group B consisted of the solvents used in the hydrolysis of TEOS step. Finally, 0.1 M HCl(aq) was used to initiate the hydrolysis reaction.

2.2. Synthesis of UAN 1000-1450

UAN 1000-1450 was synthesized via a three-step reaction process, similar to our previous study. The detailed synthetic process for UAN 1000-1450 was reported in our previous publication [22]. The Arabic numbers in the name of the UAN 1000-1450 precursor denote the molecular weights of the GP and PEG used, respectively. The molecular weight of the synthesized UAN 1000-1450 measured using a gel permeation chromatography (GPC) analysis was 38,765 g/mol, with a polydispersity of 2.1. The expected schematic structure of UAN 1000-1450 is shown in Figure 1.

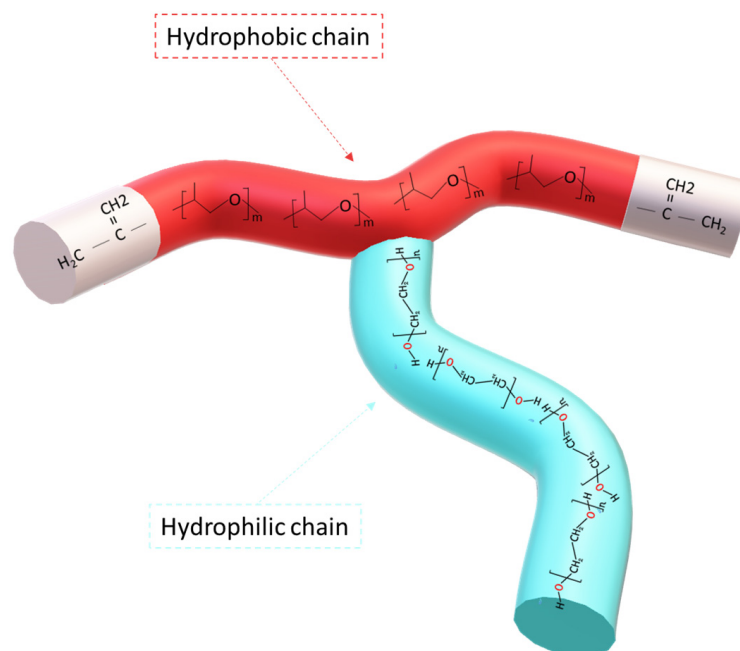


Figure 1. Schematic structure of UAN 1000-1450.

2.3. Preparation of SiO₂ Organic-Inorganic Hybrid Sols

Firstly, UAN 1000-1450 was mixed with one of the solvents from group A and polymerized in the presence of AIBN at 60 °C for 12 h. Simultaneously, the TEOS was hydrolyzed with 2.59 g of 0.1 M HCl(aq) in one of the solvents from group B at ambient temperature for the entire 12 h. The molar ratio (also known as *r* value) of H₂O to Si at this step was 0.5. Then, the hydrolyzed TEOS and the polymerized UAN solution (named poly(UAN)) were mixed and stirred at 80 °C for a further 12 h with 12.96 g of 0.1 M HCl(aq) corresponding to an *r* value of 3, to complete the hydrolysis-condensation reaction. The resulting SiO₂ O-I hybrid nanoparticles and their sols are denoted as UT10 (X-Y) nanoparticles and UT10 (X-Y) sols, respectively. The number '10' in the UT10 (X-Y) sols symbolizes the weight ratio of the TEOS to the UAN precursor, while the letters 'X' and 'Y' denote the solvent group employed during the preparation of the O-I SiO₂ hybrid nanoparticles and sols. For example, UT10 (M-E) was prepared using solvent M of group A in the polymerization step of the UAN and solvent E of group B in the hydrolysis step of the TEOS. The detailed components used in the experiment are summarized in Table 1.

2.4. Preparation of O-I SiO₂ Hybrid Coating Films on Glass Substrate

The prepared UT10 sols (with volume 0.1 mL) were coated onto a glass substrate (Marienfeld, 76 × 26 × 1 mm, Paul Marienfeld GmbH & Co.KG, Stuttgart, Germany) using a Mayer bar 13 to form a homogeneous O-I hybrid wet coating. Then, the wet coating was thermally treated at 100 °C for 30 min, followed by aging at room temperature for 3 h. The resulting samples were used to analyze the morphology (i.e., particle size and shape) and to evaluate the mechanical properties of the cured UT10 O-I hybrid coating films.

Table 1. Detailed chemical components used in the preparation of O-I hybrid SiO₂ sols.

UT10 Sols	Solvent of Group A	Weight of Solvent of Group A (g)	Solvent of Group B	Weight of Solvent of Group B (g)	Weight of UAN 1000-1450 (g)	Weight of TEOS (g)	Weight of AIBN (g)	Weight of 0.1 M HCl(aq) (g)
UT10 (M-E)	M	30	E	30	6	60	0.07	15.5
UT10 (C-E)	C	30	E	30	6	60	0.07	15.5
UT10 (E-E)	E	30	E	30	6	60	0.07	15.5
UT10 (P-E)	P	30	E	30	6	60	0.07	15.5
UT10 (M-P)	M	30	P	30	6	60	0.07	15.5
UT10 (C-P)	C	30	P	30	6	60	0.07	15.5
UT10 (E-P)	E	30	P	30	6	60	0.07	15.5
UT10 (P-P)	P	30	P	30	6	60	0.07	15.5

2.5. Characterization

A Nicolet iS5 FT-IR spectrometer (Thermo Fisher Scientific, Waltham, MA, USA) was employed in the range of 4000–400 cm⁻¹ to identify the synthesized UAN 1000-1450 precursors. Gel permeation chromatography (GPC, EcoSEC HLC-8320 GPC, Tosoh, Tokyo, Japan) was used to determine the molecular weight of UAN 1000-1450. DMF was used as the developing solvent; the sample concentration was 3 mg/mL, and the injection amount was 10 µL with a flow rate of 0.35 mL/min at 40 °C. A dynamic light scattering analyzer (DLS, Zetasizer Nano ZS, Malvern Instruments, Malvern, UK) was used to measure the particle size of the UT10 O-I hybrid nanoparticles dispersed in the solution. ²⁹Si-NMR measurements (Ascend 400 manufactured by Asahi Kasei Corporation, Tokyo, Japan) were used to investigate the degree of polymerization (the degree of the hydrolysis and condensation reaction) of SiO₂ O-I hybrid sols.

The thermal properties and the inorganic content of SiO₂ O-I hybrid coating films were determined using thermogravimetric analysis (TGA, SDT Q600 V20.5 Build 15 Universal V4.4A, TA Instruments, New Castle, DE, USA). The test was performed under a nitrogen atmosphere, at a heating rate of 10 °C min⁻¹, from ambient temperature up to 800 °C. The surface morphology of the coating films was analyzed using a field emission scanning electron microscope (FE-SEM, JEOL JSM-6701F/X-MAX, Peabody, MA, USA). A cryogenic transmission electron microscopy (cryo-TEM) experiment was performed using an FEI CryoTecnai F20 Polara device operated at 200 kV. The transmittance of the SiO₂ O-I hybrid coating films in the visible region was measured using a UV-vis spectrometer (UV-2450, Shimadzu, Kyoto, Japan) in the range of 400–800 nm. The surface hardness of the SiO₂ O-I hybrid coating films was quantified via the indentation hardness using an iMicro nanoindenter (USA), employing a continuous stiffness measurement (CSM) mode under load control with a set maximum load of 100 mN. A nanoscratch test was also performed using the iMicro instrument. This test employed a conical tip with a vertical load incrementally increased from 0.04 to 40 mN. Finally, the thickness of the SiO₂ O-I hybrid coated films was measured by averaging five readings obtained with the Digimatic micrometer MDH-25M (Mitutoyo, Kawasaki city, Japan).

3. Results and Discussion

3.1. Effect of the Solvent Type on the Colloidal Property of Silica Sols

3.1.1. Change in the Particle Size with the Type of Solvent Used in the Preparation of the Poly(UAN) Solution

Due to the structure consisting of a polypropylene oxide (PPO) chain and a polyethylene oxide (PEO) chain at the same backbone, the UAN 1000-1450 can disperse well in various types of organic solvents. In this study, the UAN 1000-1450 was mixed and polymerized in the four types of solvent mentioned, resulting in the formation of transparent solutions. To confirm the size of the poly(UAN) in the solvents, dynamic light scattering (DLS) was carried out. The formation of these dispersed nanoparticles in the organic solvent could be explained due to the difference in solubility between the PEO and PPO segments which caused microphase separation. The particle size and its corresponding polydispersity (PDI) of the PUAN solution prepared with four different solvents were

determined using DLS measurement, which are summarized in Table 2. The poly(UAN) nanoparticles exhibited a size range of 12.54 to 48.06 and a corresponding polydispersity (PDI) range of 0.2 to 0.79. As shown in Figure 2, the size of the poly(UAN) nanoparticles increased with the dielectric constant of the solvent, indicating that the size of poly(UAN) nanoparticles increased with the increase in polarity of the solvent used in the preparation. Particularly, among the four types of solvent, the poly(UAN) nanoparticles showed the largest size (48.06 nm) in ethanol, which had the highest polarity (dielectric constant of solvent of 24.5). In contrast, solvent P, having the lowest polarity (dielectric constant of solvent of 7.8), resulted in the smallest nanoparticle size of poly(UAN) (12.54 nm). The size of the poly(UAN) nanoparticles in solvent C and solvent M, which had dielectric constants of 18.2 and 18.85, respectively, were 14.68 and 19.06 nm, respectively. This could be explained due to the self-assembly mechanism of amphiphilic polymers in polar or nonpolar solvents. In a protic solvent with strong polarity like ethanol, the hydrophilic PEG chains of the amphiphilic polymer have a stronger affinity for the solvent molecules, leading to an increase in the solvation of the PEG chains. Consequently, the PEG chains were extended and occupied a larger volume, resulting in larger micellar or self-assembled structures [2,17,18,21]. In the case of aprotic solvents, such as M and C, the interaction of the hydrophobic segment of the amphiphilic polymer was favored. In higher polarity aprotic solvents, the size of the aggregates of the hydrophobic segment of poly(UAN) was increased through dispersion forces (or van der Waals forces), while the hydrophilic segment of the poly(UAN) could interact with the polar functional groups in the solvent molecules through the dipole-dipole or other polar interactions, resulting in a higher order of size of poly(UAN) nanoparticles [23,24]. Conversely, aprotic solvents with a lower polarity resulted in smaller-sized self-assembled structures.

Table 2. The particle size of poly(UAN) dispersed in four types of solvent.

Solvent Used in Polymerization of UAN	Average Nanoparticle Size of Poly(UAN) (d-nm)	Polydispersity (PDI)
P	12.54 ± 1.67	0.548
C	14.68 ± 0.4038	0.627
M	19.06 ± 1.967	0.395
E	48.06 ± 3.946	0.476

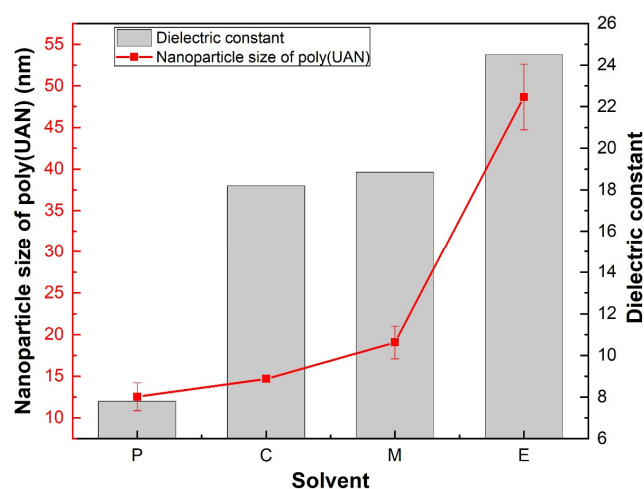


Figure 2. Effect of the dielectric constant of solvent on the particle size of poly(UAN).

The particle size of poly(UAN) in solvent C was slightly larger than that of poly(UAN) in solvent P, even though cyclohexanone has a significantly higher dielectric constant than PGME. This result could be explained by the amphiphilic backbone of poly(UAN) chains. Because of their amphiphilicity, the PPO and PEO segments of the poly(UAN)

chains could have an affinity simultaneously to various solvents having different polarities, which could result in a slight difference in the size of poly(UAN) in two solvents greatly differing in dielectric constants. Furthermore, the largest size of poly(UAN) in ethanol could be interpreted as due to the strongest interaction between the hydrophobic backbone and ethanol as well as between the hydrophilic segment and ethanol. So, it could be thought that both the hydrophilic and hydrophobic moieties have the strongest interaction with a protic polar solvent, ethanol, which resulted in the formation of the largest size of poly(UAN) in ethanol.

3.1.2. Change in the Particle Size with the Type of Solvent Mixtures Used in the Preparation of Silica Sols in the Presence of Poly(UAN) Solutions

Firstly, we tried to hydrolyze TEOS in the four solvents (C, M, P, and E). However, white precipitates formed when adding 0.1 M HCl(aq) to the mixture containing TEOS and the aprotic solvents (C and M). This occurrence could be attributed to the absence of hydrogen bonding between the aprotic solvents and hydroxyl ions, rendering the hydroxyl ions more nucleophilic. This increased the rate of the S_N2 reactions and led to the formation of more hydroxyl ions during the hydrolysis step [25]. Simultaneously, these silanols (Si-OH) might have condensed to form siloxane (Si-O-Si) bonds, resulting in the formation of larger insoluble silica particles, which appeared as white precipitates. Consequently, only the two protic solvents, E and P, were used in the hydrolysis step of TEOS.

In the preparation process of the silica sols, the poly(UAN) played a role as a stabilization agent. The stabilization mechanism is described in Figure 3. The PEG chain contains ethylene oxide moieties and a hydroxyl group at the end of the chain, which could make a hydrogen bond with the silanol group of silica during the hydrolysis-condensation reaction, preventing the aggregation of silica nanoparticles. Therefore, the difference in size of poly(UAN) in the four types of solvent might affect the size of the silica sols during the preparation process. As shown in Table 3, the size range of the silica sols varies from 11.72 nm to 33.8 nm, where the UT10 (E-E) sols show the largest particle size, while the UT10 (P-P) sols show the smallest particle size. Another trend that was observed was that the increase in the size of the particle was proportional to the increase in the polarity of the solvent used in the polymerization of UAN 1000-1450. Additionally, the particle size of the sols prepared using ethanol in the hydrolysis of TEOS step was larger than when using PGME. This difference could be explained because of the effect of the solvent on the size of the poly(UAN) and the hydrolysis of the monomer. As we mentioned before, the size of the poly(UAN) depends on the polarity of solvent; the higher dielectric constant provides the larger size of poly(UAN) particles. Furthermore, during the hydrolysis of the TEOS, using a highly polar protic solvent like ethanol accelerated the reaction rate, resulting in an increased production of silanol. Consequently, when H-TEOS was added to the poly(UAN) solution, the PEG hydrophilic tail of poly(UAN) 1000-1450 formed hydrogen bonds with the OH groups of the silanol and interacted with the polar molecules of the solvent, leading to the formation of a larger "ring" surrounding the SiO_2 nanoparticles, leading to the increase in the particle size.

On the other hand, after four months of storage at room temperature, the particle size of the UT10 sols prepared using the protic-protic solvent mixture showed significant changes in comparison to the UT10 nanoparticles prepared by the aprotic-protic solvent combination. While the particle size of the UT10 nanoparticles prepared from the C-P, P-P, and M-E solvent mixtures only slightly changed from 0.6 to 0.8 nm, the UT10 particles prepared from the protic solvents containing E-E showed a significant increase in particle size, ranging from 31.1 to 95.5 nm. According to these results, it could be said that the solvent mixture consisting of aprotic and protic solvents could provide long-term, colloidal stable nanoparticles with appropriate size.

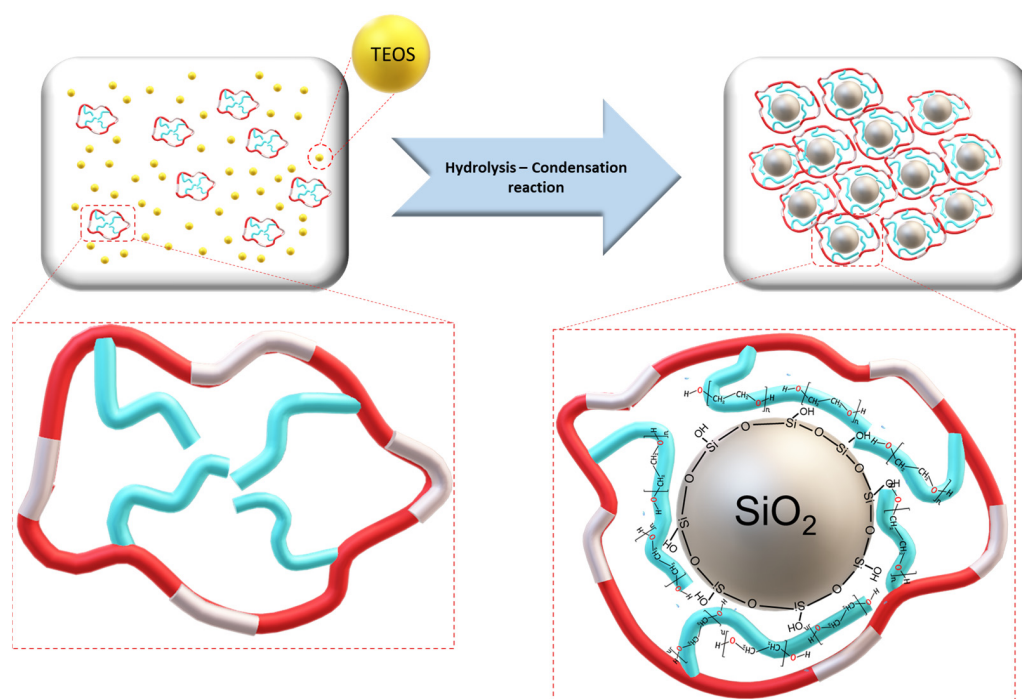


Figure 3. Stability mechanism of Poly(UAN) with silica nanoparticles.

Table 3. Size of SiO₂ sols when prepared and 4 months after preparation.

Solvent Used in Polymerization of UAN	Solvent Used in Hydrolysis of TEOS	Size of SiO ₂ Nanoparticles after Preparation (nm)	PDI of SiO ₂ Nanoparticles after Preparation	Size of SiO ₂ Nanoparticles 4 Months after Preparation (nm)	PDI of SiO ₂ Nanoparticles 4 Months after Preparation
P	P	11.72 ± 0.04	0.357	12.09 ± 0.49	0.549
	E	14.56 ± 0.46	0.503	20.10 ± 0.59	0.385
C	P	15.85 ± 0.03	0.403	15.29 ± 0.06	0.5
	E	19.28 ± 0.1	0.455	21.84 ± 0.08	0.447
M	P	16.05 ± 0.07	0.283	17.75 ± 0.3	0.52
	E	22.13 ± 0.17	0.294	22.93 ± 0.04	0.27
E	P	16.99 ± 0.06	0.493	48.1 ± 3.94	0.793
	E	33.8 ± 0.7	0.318	129.3 ± 11.5	0.527

3.2. Effect of the Solvent Type on the Reaction in the Preparation of Silica Sols

3.2.1. Effect of the Solvent Type on the Degree of Condensation (DOC) Reaction of TEOS

The TEOS was converted to SiO₂ O-I hybrid nanoparticles via a hydrolysis-condensation reaction. The presence of an acid catalyst, HCl, promoted the hydrolysis of TEOS, leading to the generation of silanol groups (Si-OH) and ethanol as a byproduct. Subsequently, the silanol groups formed siloxane (Si-O-Si) crosslinks during the condensation reaction, resulting in the formation of the silica network. During the reaction, the solvent was used not only to dissolve the monomers but also to increase the reaction rate by providing the needed ions for the medium condition. For example, protic solvents favor acid-catalyzed hydrolysis by rendering the H₃O⁺ ions more electrophilic. In contrast, nonprotic solvents accelerate the basic-catalyzed hydrolysis by rendering the OH⁻ ions more nucleophilic. Compared to other studies using a single solvent during the hydrolysis-condensation reaction, using solvent mixtures, especially combining polar aprotic solvent and polar protic solvents, provided high efficiency, which was indicated via the degree of condensation (DOC). A higher DOC could lead to the formation of a more densely crosslinked siloxane

bond (Si-O-Si) and a denser network structure in the film, since it could increase the degree of crosslinking of the alkoxy silane compound, resulting in the coating film becoming stronger, more rigid, and more resistant to deformation. In this study, four types of UT10 sols with different solvent mixtures were prepared to measure the DOC using ^{29}Si -NMR analysis, including UT10 (M-E), UT10 (C-P), UT10 (E-E), and UT10 (E-P).

^{29}Si -NMR analysis is known as an effective tool to confirm the formation of a siloxane network, which is evidenced by the existence of the highly condensed Si species shown in Figure 4. The degree of condensation was calculated using the following equation [26]:

$$\text{The degree of condensation (DOC)} = \frac{Q^1 + 2Q^2 + 3Q^3 + 4Q^4}{4(Q^1 + Q^2 + Q^3 + Q^4)} \times 100\% \quad (1)$$

where Q^n denotes the silicon from tetrafunctional alkoxy silanes, denoted as $\text{Si}(\text{OR})_4$, such as TEOS. The letter “n” indicates the number of siloxane bonds of silicon. The ^{29}Si chemical shifts demonstrated at -91 ppm, -100 ppm, and -110 ppm correspond to the peaks of the $\text{Si}(\text{OSi})_4$ for the Q^4 , $\text{Si}(\text{OSi})_3\text{OH}$ for the Q^3 , and $\text{Si}(\text{OSi})_2(\text{OH})_2$ for the Q^2 groups, respectively [27].

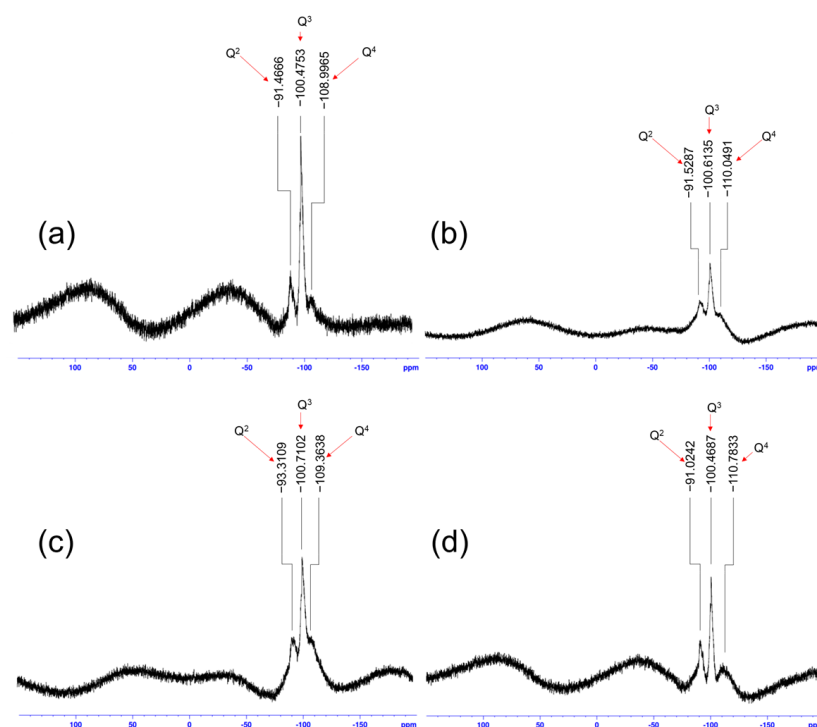


Figure 4. ^{29}Si -NMR spectra of (a) UT10 (C-P) solution, (b) UT10 (E-P) solution, (c) UT10 (M-E) solution, and (d) UT10 (E-E) solution.

Figure 4 shows the ^{29}Si -NMR spectrum for each of the UT10 sols after the hydrolysis-condensation reaction. The signal of species and the relative intensity of the four UT10 sols are summarized in detail in Table 4. As can be seen, the observation of the Q^2 , Q^3 , and Q^4 species in the four UT10 sols indicated a highly efficient conversion of silicon species. Among the observed species, the Q^3 species were predominant, whereas the Q^4 species were only present in a small amount. However, the appearance of the Q^4 species implied the formation of a condensed siloxane network with a high degree of condensation. The degree of condensation was calculated following Equation (1) and is shown in Table 3.

Table 4. Relative peak intensity from the deconvolution of the ^{29}Si -NMR spectra.

Samples	Chemical Shift of Peak (ppm)				Relative Peak Intensity (%)				DOC (%)
	Q ¹	Q ²	Q ³	Q ⁴	Q ¹	Q ²	Q ³	Q ⁴	
UT10 (M-E)	---	−93.31	−100.71	−109.35	0	20.7	58.74	20.56	75.11
UT10 (E-E)	---	−91.02	−100.47	−110.78	0	24.15	68.74	7.1	71.95
UT10 (C-P)	---	−91.47	−100.47	−108.99	0	17.69	77.4	4.9	71.8
UT10 (E-P)	---	−91.53	−100.61	−110.05	0	26.46	59.24	14.3	72.94

The degree of condensation (DOC) in the four UT10 sols showed slight differences, with UT10 (M-E) having the highest DOC at over 75% and UT10 (E-P) having the lowest DOC of 70.74%. UT10 (E-E) and UT10 (C-P) had DOC values of 71.95% and 71.8%, respectively. The highest DOC, the one of UT10 (M-E), might be explained by the effect of the combination of the highly polar aprotic solvent (MEK) and the highly polar protic solvent (ethanol) on the hydrolysis-condensation reaction, which could be explained as follows: During the hydrolysis of TEOS under acidic-catalyzed conditions, the alkoxide group (−OR) was protonated by the presence of H_3O^+ hydronium ions (formed through the interaction of H^+ and water molecules). The water molecule attacked from the rear and acquired a partial positive charge, while the alkoxide was protonated, making alcohol a better leaving group. Therefore, hydrolysis took place rapidly, forming intermediate species containing Si-OH groups known as silanols. This reaction followed the nucleophilic substitution $\text{S}_{\text{N}}2$ -Si mechanism, which in the present study generally occurred more quickly in polar aprotic solvents than in polar protic solvents, as the polar aprotic solvents lacked hydrogen atoms that could participate in hydrogen bonding with the nucleophile or the leaving group. This absence of strong hydrogen bonding allowed the nucleophile to attack the substrate more easily, leading to a faster $\text{S}_{\text{N}}2$ reaction rate. However, as we mentioned before, the polar protic solvent not only made hydronium ions more electrophilic (shown in Figure 5) but also played important roles by providing hydrogen bonds with silanol groups, which could help them disperse in solution, preventing rapid condensation and precipitation. As a result, it might be said that the presence of combined aprotic and protic solvents could make the hydrolysis reaction happen faster and form more hydroxyl groups while keeping the particles dispersed in the solution.

In condensation reactions under acid-catalyzed conditions, a highly polar protic solvent such as ethanol could enhance the degree of condensation through the formation of a dense siloxane bond [28], because as the reaction progresses, the acid catalyst protonates silanol (Si-OH) species. This protonation renders the silicon atom more electrophilic, making it highly susceptible to nucleophilic attacks by neighboring hydroxyl groups. The protic solvent, through its ability to engage in hydrogen bonding and facilitate protonation, enhances the reactivity of the silanol groups. Thus, the protic solvent's role in this context is to enhance the electrophilic nature of silicon and catalyze the efficient condensation of silanol groups. Considering these complex mechanisms, using a combination of highly polar aprotic-protic solvents, such as M-E, during the hydrolysis-condensation of TEOS under acidic-catalyst conditions showed a synergistic effect. This combination enhances the hydrolysis rate, stabilizes the reactive species, and facilitates effective hydrolysis and condensation reactions.

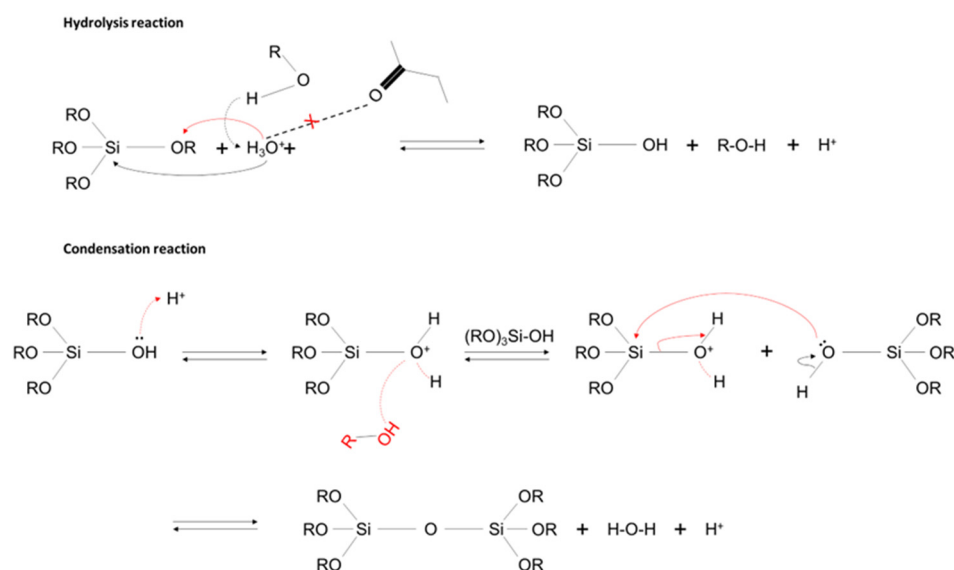


Figure 5. Mechanisms of acid-catalyzed hydrolysis and condensation of TEOS, and the role of the solvent during reaction.

3.2.2. Mechanical Strength of Coated Films Formed by Various Silica Sols Prepared Using Different Solvent Mixtures

Figure 6 illustrates the formation mechanism of UT10 hybrid coating films via the sol-gel process. In the sol state, the colloidal UT10 hybrid nanoparticles dispersed in solvent mixtures were stabilized by the action of the hydrophilic PEG chain located on the outer shell. After the coating solution was placed on the substrate, during the thermal curing process, the UT10 hybrid nanoparticles were closely packed owing to the evaporation of the solvent, and the postcondensation reaction occurred among the alkoxide groups to enable the UT10 sols to become solid O-I hybrid nanoparticles. Therefore, this process was named the sol-gel process. During this process, closely packed hybrid nanoparticles were converted to solid nanoparticles connected by the organic component poly(UAN), forming continuous films on the substrates. Therefore, it could be said that during thermal curing, the poly(UAN) played dual roles: preventing macro-scale particle growth and facilitating the formation of continuous films, resulting in the improved mechanical properties of the coating film.

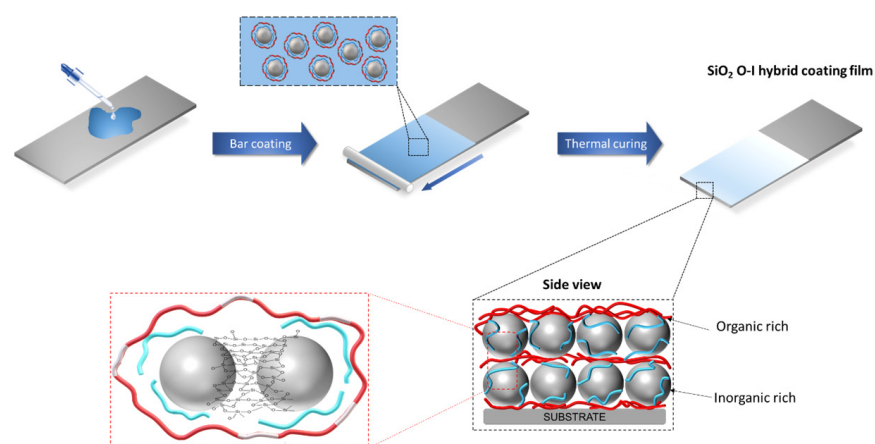


Figure 6. The formation of UT10 O-I hybrid coating films via the sol-gel process.

Figure 7a–d shows the FE-SEM images of four types of UT10 hybrid coating films formed on glass slides. All the UT10 coating films exhibited the formation of closely packed spherical nanoparticles, resulting in the formation of a continuous silica matrix. The

morphology of the coating particles was characterized using cryo-TEM to observe smaller details, as shown in Figure 7e. The size of the silica particles after thermal curing was 10–12 nm, which was smaller than the silica particles dispersed in their sols, which may have led to the high transparency of the coating film in the visible range of 400–800 nm with the average transmittance over 90%, stemmed from UV-vis spectra (as shown in Figure 8).

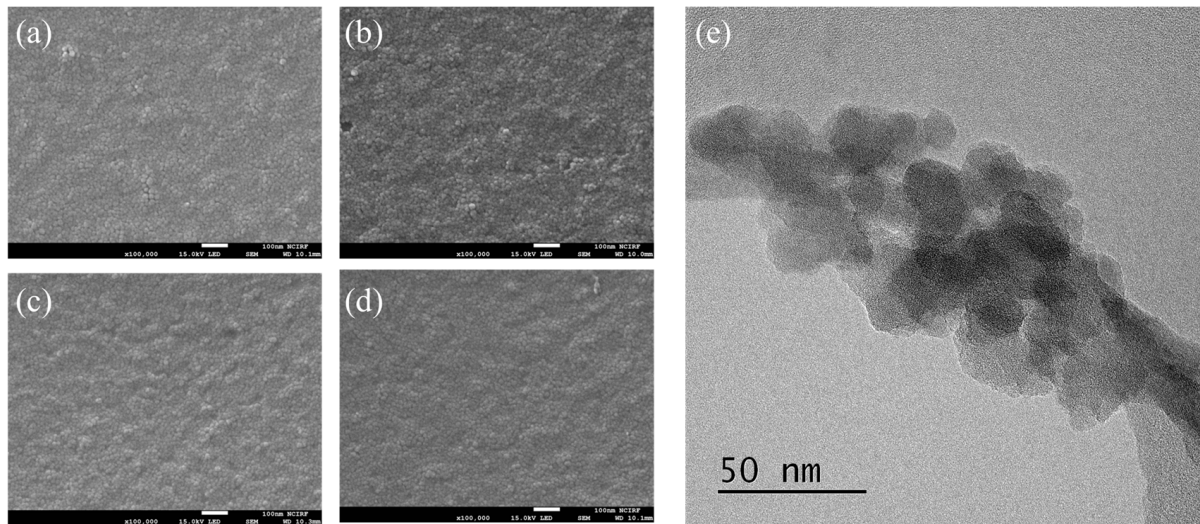


Figure 7. FE-SEM images of the thermally cured UT10 hybrid coating films formed on glass substrates: (a) UT10 (E-P), (b) UT10 (C-P), (c) UT10 (E-E), (d) UT10 (M-E), and (e) cryo-TEM image of UT10 (M-E) hybrid coating.

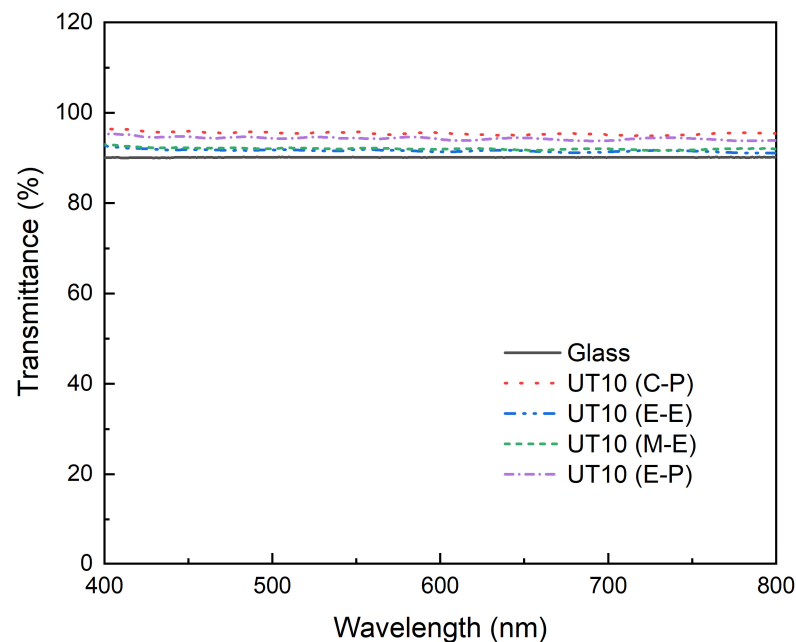


Figure 8. Optical transmittances of UT10 hybrid coating films on glass substrate.

As discussed earlier, the solution with a higher DOC value showed higher hardness of the resulting coating film due to the denser siloxane bonds within the coating network. On the other hand, it also implied a higher proportion of inorganic content in this solution. This hypothesis was confirmed via TGA characterization, as shown in Figure 9. The TGA results showed the inorganic content after the complete decomposition of the organic component from the cured coating film (after 600 °C). All the cured UT10 coating films retained 65%–73% of their initial weight at 800 °C, indicating a high amount of inorganic

content in them. Specifically, the UT10 (M-E), having the highest DOC value, indicated the more extensive condensation of silanol groups into inorganic siloxane bonds, leading to highest inorganic content in the coating film. Conversely, the UT10 (C-P) showed the lowest inorganic content due to its DOC value being the lowest.

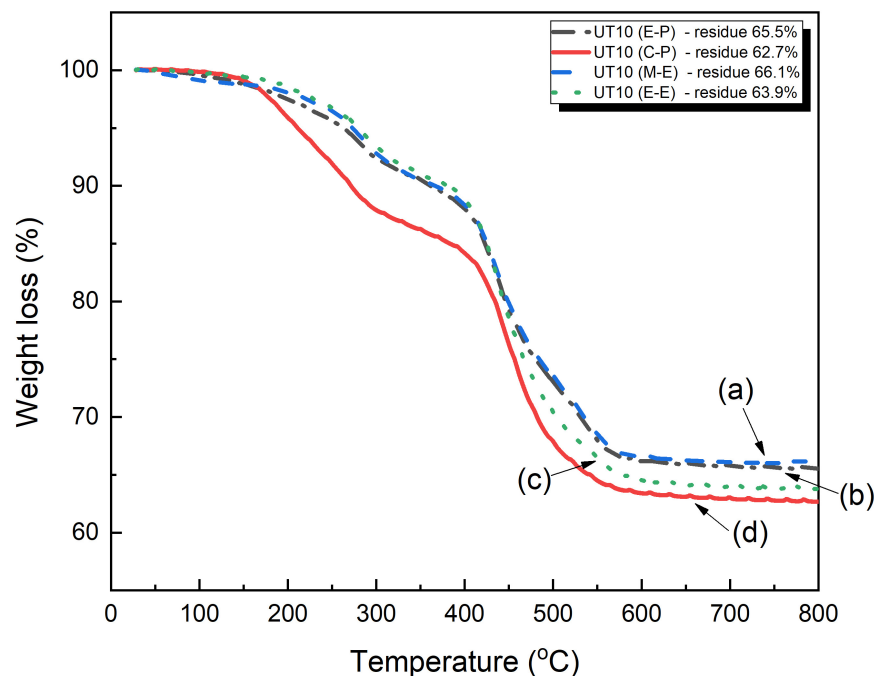


Figure 9. TGA results of the cured UT10 solid films prepared using different combinations of solvents: (a) UT10 (M-E), (b) UT10 (E-P), (c) UT10 (E-E), and (d) UT10 (C-P).

To evaluate the relationship between the hardness of the UT10 coating films and their DOC, we performed nanoindentation experiments based on the Oliver-Pharr method. Figure 10a shows the nanoindentation load-displacement curves of the coating films prepared using UT10 sols with different solvent mixtures, and Figure 10b shows the relationship between the DOC of the UT10 sols and their hardness value. The solutions with a higher degree of condensation showed a smaller hysteresis of the load-displacement curve (revealing the higher elastic resilience) and a higher nanoindentation hardness. The UT10 (M-E), with the highest DOC, showed a remarkable hardness of up to 0.97 GPa and the smallest hysteresis of the load-displacement curve with a film thickness of 4.76 μm . The UT10 (E-E) had a hardness of 0.74 GPa (thickness 7.16 μm), and the UT10 C-P (thickness 6.07 μm) had a hardness of 0.63 GPa, even though they had almost similar DOC values. This result could be attributed to the boiling point of the solvent combination used in the solution preparation process. Cyclohexanone and PGME had high boiling points of 155.6 $^{\circ}\text{C}$ and 120 $^{\circ}\text{C}$, respectively. Hence, under the curing condition of 100 $^{\circ}\text{C}$ for 30 min, the solvents were not completely removed. This incomplete removal led to a less densely packed structure, reducing the crosslinking density within the network, consequently resulting in a lower mechanical strength of the coating film. This outcome indicated that the hardness of the O-I hybrid coating film was strongly dependent on the degree of crosslinking (DOC) and the inorganic content. Furthermore, it is believed that the solvents played a significant role in the preparation of the silica sols and the mechanical strength of their coating films via the solvent's effect on the degree of condensation and the curing process.

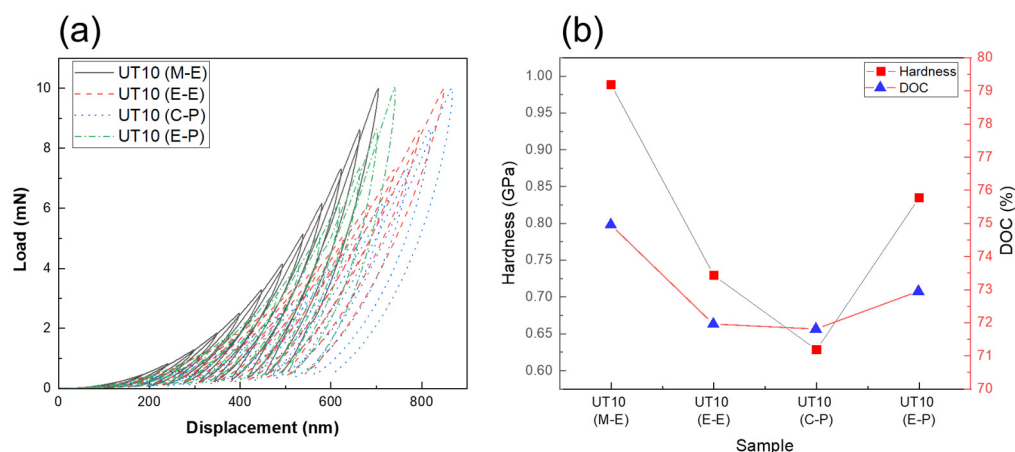


Figure 10. (a) The nanoindentation load-displacement curves of the coating films prepared using UT10 sols with different solvent mixtures and (b) The relationship between the DOC and hardness of the UT10 hybrid coating films using different combinations of solvents.

4. Conclusions

In summary, the effect of solvents on the degree of condensation in the preparation of colloidal stability O-I hybrid nanoparticles via the hydrolysis-condensation reaction and the performance of the coating films were investigated. The study findings indicated that using a highly polar aprotic-protic solvent mixture can significantly increase the condensation degree under acidic-catalyzed conditions. This is because the strong polar aprotic solvent facilitated the S_N2 mechanism-based hydrolysis reaction quickly, while the high polar protic solvent formed hydrogen bonds with silanol groups, stabilizing their dispersion in the solution and making the hydronium ions more electrophilic. As a result, this led to an overall improvement in the efficiency of the hydrolysis reaction. Additionally, in the condensation reaction, using a strong polar protic solvent could generate the electrophilic nature of silicon, catalyzing the efficient condensation of silanol groups. By comprehending these mechanisms of both aprotic and protic solvents in hydrolysis-condensation under acidic-catalyzed conditions, we successfully prepared UT10 nanoparticles characterized by a high degree of condensation and exceptional stability, maintaining their colloidal state for at least four months, even at high nanoparticle concentrations exceeding 40%. All UT10 sols showed the appearance of Q^4 species, and the UT10 (M-E) prepared from the strong polar aprotic and protic solvents showed excellent hardness (more than 0.9 GPa with a minimal coating thickness of 4.76 μm). Furthermore, considering solvent boiling points was crucial in influencing the evaporation rates and subsequently impacting the coating hardness. Thus, by understanding the distinct contributions of each solvent, we can optimize the sol-gel process for diverse applications, offering a versatile and practical approach to industrial coating design.

Author Contributions: Conceptualization, J.K.; methodology, J.K. and H.N.L.; validation, H.N.L. and C.L.; writing—original draft preparation, H.N.L.; writing—review and editing, J.K.; supervision, J.K.; project administration, C.L., W.J. and J.K.; funding acquisition. All authors have read and agreed to the published version of the manuscript.

Funding: This research was supported by “Regional Innovation Strategy (RIS)” through the National Research Foundation of Korea (NRF) funded by the Ministry of Education (MOE) (2022RIS-005).

Institutional Review Board Statement: Not applicable.

Informed Consent Statement: Not applicable.

Data Availability Statement: The data presented in this study are available on request from the corresponding author.

Acknowledgments: We thank our colleagues for their contributions to this work.

Conflicts of Interest: Authors Choonho Lee and Woo Chul Jung were employed by Hyundai Motor Company. The remaining authors declare that the research was conducted in the absence of any commercial or financial relationships that could be construed as a potential conflict of interest.

References

1. Karg, M.; Lu, Y.; Carbó-Argibay, E.; Pastoriza-Santos, I.; Pérez-Juste, J.; Liz-Marzán, L.M.; Hellweg, T. Multiresponsive Hybrid Colloids Based on Gold Nanorods and Poly(NIPAM-co-allylactic acid) Microgels: Temperature- and pH-Tunable Plasmon Resonance. *Langmuir* **2009**, *25*, 3163–3167. [[CrossRef](#)]
2. Willander, M.; Nur, O.; Zaman, S.; Zainelabdin, A.; Bano, N.; Hussain, I. Zinc oxide nanorods/polymer hybrid heterojunctions for white light emitting diodes. *J. Phys. D Appl. Phys.* **2011**, *44*, 224017. [[CrossRef](#)]
3. Wei, Y.-X.; Deng, C.; Wei, W.-C.; Chen, H.; Wang, Y.-Z. Hybrid Nanorods Composed of Titanium, Silicon, and Organophosphorus as Additives for Flame-Retardant Polycarbonate. *ACS Appl. Nano Mater.* **2019**, *2*, 4859–4868. [[CrossRef](#)]
4. Liu, B.-T.; Hung, T.-Y.; Gorji, N.E.; Mosavi, A.H. Fabrication and characterization of Cesium-doped Tungstate nanorods for Near-Infrared light absorption in dye sensitized solar cells. *Results Phys.* **2021**, *29*, 104804. [[CrossRef](#)]
5. Chen, W.; Wu, W.; Pan, Z.; Wu, X.; Zhang, H. PEG400-assisted synthesis of oxygen-incorporated MoS₂ ultrathin nanosheets supported on reduced graphene oxide for sodium ion batteries. *J. Alloys Compd.* **2018**, *763*, 257–266. [[CrossRef](#)]
6. Islam, S.; Bidin, N.; Riaz, S.; Naseem, S.; Marsin, F.M. Correlation between structural and optical properties of surfactant assisted sol-gel based mesoporous SiO₂-TiO₂ hybrid nanoparticles for pH sensing/optochemical sensor. *Sens. Actuators B Chem.* **2016**, *225*, 66–73. [[CrossRef](#)]
7. Luo, M.; He, Y.; Chen, Q.; Li, C. Synthesis and Structural and Electrical Characteristics of Polypyrrole Nanotube/TiO₂ Hybrid Composites. *J. Macromol. Sci. Part B* **2010**, *49*, 419–428. [[CrossRef](#)]
8. Lee, H.; Kim, S.; Kim, W.; Kang, S.-M.; Kim, Y.H.; Jang, J.; Han, S.M.; Bae, B.-S. Highly transparent and resilient urethane-methacrylate siloxane composite for hard, yet stretchable protective coating. *Prog. Org. Coat.* **2022**, *162*, 106567. [[CrossRef](#)]
9. Ahmad, S.; Zafar, F.; Sharmin, E.; Garg, N.; Kashif, M. Synthesis and characterization of corrosion protective polyurethane-fattyamide/silica hybrid coating material. *Prog. Org. Coat.* **2012**, *73*, 112–117. [[CrossRef](#)]
10. Li, P.; Guo, W.; Lu, Z.; Tian, J.; Li, X.; Wang, H. UV-responsive single-microcapsule self-healing material with enhanced UV-shielding SiO₂/ZnO hybrid shell for potential application in space coatings. *Prog. Org. Coat.* **2021**, *151*, 106046. [[CrossRef](#)]
11. Eshaghi, A. Transparent hard self-cleaning nano-hybrid coating on polymeric substrate. *Prog. Org. Coat.* **2019**, *128*, 120–126. [[CrossRef](#)]
12. Škoc, M.S.; Macan, J.; Pezelj, E. Modification of polyurethane-coated fabrics by sol-gel thin films. *J. Appl. Polym. Sci.* **2014**, *131*, 39914. [[CrossRef](#)]
13. Bail, N.L.; Benayoun, S.; Toury, B. Mechanical properties of sol-gel coatings on polycarbonate: A review. *J. Sol-Gel Sci. Technol.* **2015**, *75*, 710–719. [[CrossRef](#)]
14. Figueira, R.B.; Silva, C.J.R.; Pereira, E.V. Organic-inorganic hybrid sol-gel coatings for metal corrosion protection: A review of recent progress. *J. Coat. Technol. Res.* **2015**, *12*, 1–35. [[CrossRef](#)]
15. Kim, N.; Li, X.; Kim, S.H.; Kim, J. Colloidally stable organic-inorganic hybrid nanoparticles prepared using alkoxy silane-functionalized amphiphilic polymer precursors and mechanical properties of their cured coating film. *J. Ind. Eng. Chem.* **2018**, *68*, 209–219. [[CrossRef](#)]
16. Bari, A.H.; Jundale, R.B.; Kulkarni, A.A. Understanding the role of solvent properties on reaction kinetics for synthesis of silica nanoparticles. *Chem. Eng. J.* **2020**, *398*, 125427. [[CrossRef](#)]
17. Zerda, T.W.; Hoang, G. Effect of solvents on the hydrolysis reaction of tetramethyl orthosilicate. *Chem. Mater.* **1990**, *2*, 372–376. [[CrossRef](#)]
18. Jiang, H.; Zheng, Z.; Li, Z.; Wang, X. Effects of Temperature and Solvent on the Hydrolysis of Alkoxy silane under Alkaline Conditions. *Ind. Eng. Chem. Res.* **2006**, *45*, 8617–8622. [[CrossRef](#)]
19. Artaki, I.; Zerda, T.W.; Jonas, J. Solvent effects on the condensation stage of the sol-gel process. *J. Non-Cryst. Solids* **1986**, *81*, 381–395. [[CrossRef](#)]
20. Mandić, V.; Kurajica, S. The influence of solvents on sol-gel derived calcium aluminate. *Mater. Sci. Semicond. Process.* **2015**, *38*, 306–313. [[CrossRef](#)]
21. Bernards, T.N.M.; van Bommel, M.J.; Boonstra, A.H. Hydrolysis-condensation processes of the tetra-alkoxy silanes TPOS, TEOS and TMOS in some alcoholic solvents. *J. Non-Cryst. Solids* **1991**, *134*, 1–13. [[CrossRef](#)]
22. Kim, J.-Y.; Shin, D.-H.; Ihn, K.-J.; Suh, K.-D. Amphiphilic Polyurethane-co-polystyrene Network Films Containing Silver Nanoparticles. *J. Ind. Eng. Chem.* **2003**, *9*, 37–44.
23. Kumar, L.; Horechyy, A.; Bittrich, E.; Nandan, B.; Uhlmann, P.; Fery, A. Amphiphilic Block Copolymer Micelles in Selective Solvents: The Effect of Solvent Selectivity on Micelle Formation. *Polymers* **2019**, *11*, 1882. [[CrossRef](#)] [[PubMed](#)]
24. Mandal, P.; Mukherjee, M.; Shunmugam, R. Effect of the aqueous-organic solvent mixtures upon super-aggregation of chitosan. *J. Polym. Res.* **2023**, *30*, 9. [[CrossRef](#)]
25. Brinker, C.J.; Scherer, G.W. (Eds.) CHAPTER 3—Hydrolysis and Condensation II: Silicates. In *Sol-Gel Science*; Academic Press: San Diego, CA, USA, 1990; pp. 96–233. [[CrossRef](#)]

26. Mohseni, M.; Bastani, S.; Jannesari, A. Influence of silane structure on curing behavior and surface properties of sol–gel based UV-curable organic–inorganic hybrid coatings. *Prog. Org. Coat.* **2014**, *77*, 1191–1199. [[CrossRef](#)]
27. Glaser, R.H.; Wilkes, G.L.; Bronnimann, C.E. Solid-state ²⁹Si NMR of TEOS-based multifunctional sol-gel materials. *J. Non-Cryst. Solids* **1989**, *113*, 73–87. [[CrossRef](#)]
28. Brinker, C.J. Hydrolysis and condensation of silicates: Effects on structure. *J. Non-Cryst. Solids* **1988**, *100*, 31–50. [[CrossRef](#)]

Disclaimer/Publisher’s Note: The statements, opinions and data contained in all publications are solely those of the individual author(s) and contributor(s) and not of MDPI and/or the editor(s). MDPI and/or the editor(s) disclaim responsibility for any injury to people or property resulting from any ideas, methods, instructions or products referred to in the content.